

A global climatology of monsoon low-pressure systems

John V. Hurley* and William R. Boos

Department of Geology and Geophysics, Yale University, New Haven, CT, USA

*Correspondence to: J. V. Hurley, Department of Atmospheric and Environmental Sciences, ES351, University at Albany, Albany, NY 12222, USA.

E-mail: jvhurley12@gmail.com

The first global climatology of monsoon low-pressure systems is presented here, based on the ERA-Interim reanalysis. Low-pressure systems are classified into three intensity categories and particular focus is given to systems in the category corresponding to a traditional definition of monsoon depressions. Vortex tracks are identified using an automated algorithm applied to the distributions of 850 hPa relative vorticity, sea-level pressure and surface wind speed for 1979–2012. Roughly two to three times as many monsoon low-pressure systems form in the Northern Hemisphere as in the Southern Hemisphere during local summer. The frequency of genesis typically peaks in local summer, but low-pressure systems form throughout the year in every monsoon region. Interannual variability is weak, with standard deviations of summer counts typically being below 10% of the long-term summer mean. Regional composites reveal that monsoon depressions in India, the western Pacific and northern Australia share a common structure, consisting of a warm-over-cold core and a top-heavy column of potential vorticity that extends from the surface to the upper troposphere. A separate class of monsoon low-pressure systems develops over dry regions of West Africa and western Australia, with a shallow composite structure having a warm core in the lower troposphere and cyclonic potential vorticity confined to a thin near-surface layer. Low-pressure systems in nearly all monsoon regions are estimated to account for a large fraction, from about 40% to more than 80%, of summer precipitation on the poleward edge of the climatological mean precipitation maxima.

Key Words: monsoon depression; monsoon low-pressure system; vortex tracking

Received 24 April 2014; Revised 13 August 2014; Accepted 1 September 2014; Published online in Wiley Online Library 28 October 2014

1. Introduction

Synoptic-scale low-pressure systems play a central role in the meteorology of monsoon climates. West African monsoon rainfall is modulated by African easterly waves, which can evolve into Atlantic hurricanes (Frank, 1970; Reed *et al.*, 1977). The Indian and Australian monsoons are home to monsoon depressions, which produce a large fraction of continental summer rainfall in those regions (Yoon and Chen, 2005; Berry *et al.*, 2012). Disturbances called monsoon depressions are also observed in the western Pacific, where they frequently serve as precursors for tropical cyclones (Briegel and Frank, 1997).

The study of synoptic-scale monsoon low-pressure systems has its longest history in India, where well over a century of literature exists on the subject of monsoon depressions (Pidington, 1876; Eliot, 1890). Indian monsoon depressions are well known for forming over the Bay of Bengal and the Ganges River plain, then migrating west–northwest over northern India. These storms have outer diameters of about 2000 km, precipitating convection west–southwest of the vortex centre and cyclonic winds that peak above the surface in the lower troposphere. They are a subset of a more general distribution of synoptic low-pressure systems;

the India Meteorological Department (IMD) defines a monsoon depression as having maximum sustained surface wind speeds of 8.5–13.4 m s⁻¹, with weaker systems categorized as ‘lows’ and stronger systems as ‘deep depressions’ or ‘cyclonic storms’ (IMD, 2003). The lifetime of a typical Indian monsoon low-pressure system is about 3–6 days, and on average about 14 are commonly cited to occur each summer, of which roughly half are depressions (Godbole, 1977; Mooley and Shukla, 1987).

Storms called monsoon depressions also occur in Australia, the southwestern Indian Ocean and the western Pacific, but it is unclear whether all of these are essentially the same dynamical phenomenon. Case studies suggest that the dynamical structure of Australian monsoon depressions is similar to that of Indian monsoon depressions (e.g. Davidson and Holland, 1987). In the southwest Indian Ocean, Baray *et al.* (2010) estimate that about 5% of the approximately 8–15 tropical cyclones per year qualify as monsoon depressions, with structures similar to those observed in the Indian monsoon. The Joint Typhoon Warning Center (JTWC) defines monsoon depressions as cyclonic vortices with diameters of the order of 1000 km, light-wind cores and a loosely organized cluster of deep convection without a distinct cloud system centre (Aldinger and Stapler, 1998). By this definition,

monsoon depressions in the western Pacific are abundant: Beattie and Elsberry (2012) documented 44 cases in the summer of 2009. In Africa, many monsoon low-pressure systems go by the distinct name of easterly waves. The horizontal scale of African easterly waves is perhaps 50% larger than that of Indian monsoon depressions and the vertical structures of African easterly waves exhibit much stronger tilts than those of monsoon depressions (e.g. Godbole, 1977; Kiladis *et al.*, 2006). To our knowledge, a detailed comparison of the structures and track distributions of African easterly waves and monsoon depressions in India, Australia and the western Pacific has not been conducted.

The comparison of low-pressure systems in different monsoon regions is hampered by the fact that previous studies were limited to specific regions and used highly distinct methodologies for identifying these systems. The IMD maintains track datasets for Indian monsoon depressions that extend back to the year 1877 and were compiled operationally each year with evolving observational networks and analysis methods. Mooley and Shukla (1987) inspected weather charts published by the IMD manually and compiled tracks of Indian monsoon low-pressure systems back to the year 1888. Chen and Weng (1999) and Yoon and Chen (2005) identified Indian monsoon depressions using time-filtered streamline charts and surface pressure tendencies from reanalysis data, combined with satellite-derived outgoing long-wave radiation. African easterly waves were identified by Thorncroft and Hodges (2001) using an automated algorithm to track vorticity maxima on pressure surfaces in a reanalysis dataset. Tracks of Australian monsoon low-pressure systems were compiled by Berry *et al.* (2012) using an automated algorithm to track potential vorticity (PV) maxima on isentropic surfaces in a different reanalysis product. Although some western Pacific monsoon depressions are contained in the best track archive of the Joint Typhoon Warning Center, this seems to be a small fraction of the total and we know of no other long-term climatology of western Pacific monsoon depressions. In summary, no global inventory of monsoon low-pressure systems exists and comparing regional inventories is problematic due to their different identification criteria and underlying datasets.

The goal of this study is to create such a global inventory and use it to determine whether synoptic-scale disturbances share similar structures and track distributions across various monsoon regions. In particular, we present a climatology of monsoon low-pressure systems as they are represented in the latest reanalysis of the European Centre for Medium-Range Weather Forecasts (ERA-Interim: Dee *et al.*, 2011). Our methodology classifies low-pressure systems occurring globally in monsoon regions using intensity categories defined by the IMD, which have also been adopted by a World Meteorological Organization panel on tropical cyclones (WMO, 2011). The resulting track dataset is then analyzed to obtain seasonal cycles and interannual time series of storm counts, geographic distributions of genesis locations and composite dynamical structures, all of which are compared across the various regional monsoons. Unlike almost all previous compilations of monsoon low-pressure system tracks, our track climatology is furthermore made publicly available in electronic form (from the website of the second author, W. Boos). While we present some results for all intensity categories, we conduct the most in-depth analyses of vortices in the intensity category corresponding to monsoon depressions; this is the category for which there exists the most extensive body of literature for comparison, in the context of Indian monsoon depressions.

This study is complementary to the analysis of Lau and Lau (1990), who used seven years of early operational atmospheric analyses to examine the global distribution of tropical synoptic-scale transients. They found enhanced synoptic-scale variance in 850 hPa vorticity in many of the monsoon regions examined here and associated much of this variability with propagating wave-like disturbances. Here we take a vortex-centred approach, consistent with many of the previous tracking studies referenced above, to create a much longer climatology of monsoon low-pressure

systems and vortex-centred composites of depression-strength storms.

The next section of this article describes the data used in this investigation, the tracking algorithm and the compositing approach. Section 3 validates our results by comparing them with those of previously compiled track climatologies for India. Also presented in section 3 are genesis and track-density spatial distributions, time series of storm counts and composite dynamical structures. A synthesis of the results and a discussion of some outstanding issues are presented in section 4.

2. Data and methods

2.1. Data sources

To identify monsoon low-pressure systems, we use ERA-Interim (Dee *et al.*, 2011) six-hourly output at 0.7° horizontal resolution. Low-pressure systems are identified and categorized, as described below, using ERA-Interim 850 hPa relative vorticity, mean sea-level pressure and surface (10 m) horizontal wind speed. Composite vertical structures of monsoon depressions are obtained from ERA-Interim winds, PV and potential temperature. We also produce composites of rain-gauge and satellite-merged daily precipitation from the 1° Global Precipitation Climatology Project (GPCP: Adler *et al.*, 2003) and 2.5° daily outgoing long-wave radiation (OLR) from the National Oceanic and Atmospheric Administration (NOAA: Liebmann and Smith, 1996).

We compare our results with previously compiled sets of low-pressure system tracks for the Indian monsoon compiled by Sikka (2006) and Mooley and Shukla (1987), which cover the time periods 1984–2003 and 1888–1983, respectively. Hereafter, this track climatology will be referred to as the Sikka archive. It was obtained in article form from the library of the Center for Ocean–Land–Atmosphere Studies in Calverton, Maryland.

2.2. Tracking and compositing methods

2.2.1. TRACK

Feature tracks are identified using an automated tracking algorithm, the TRACK program (Hodges, 1995, 1999), applied to the 850 hPa relative vorticity for 1979–2012. The program was used to identify relative vorticity maxima, or minima in the Southern Hemisphere, above a threshold amplitude of $0.5 \times 10^{-5} \text{ s}^{-1}$ and then trace the feature in time and spherical latitude–longitude. Once a relative vorticity extremum is identified, the program works by minimizing a cost function for the speed and direction of motion in six-hourly reanalysis output (Hodges, 1994). This program and technique have been used in a variety of studies to identify such features as monsoon low-pressure systems, storm tracks and African easterly waves in reanalyses (Thorncroft and Hodges, 2001; Hodges *et al.*, 2003). Also, TRACK has been used to identify monsoon depressions using sea-level pressure and relative vorticity fields from general circulation model (GCM) output (Sabre *et al.*, 2000).

2.2.2. Post-TRACK processing

Results from the TRACK program are filtered further using multiple criteria. We wish to focus on tracks in monsoon regions and exclude midlatitude storms from our analysis and use the simple approach of including tracks that have at least one point inside a predefined monsoon region. While many approaches have been used to define monsoon regions (Wang and Ding, 2006), here we find the climatological mean 850 hPa temperature maximum during local summer (JJA and DJF in the Northern and Southern Hemispheres, respectively) and specify the poleward bound of the monsoon domain as lying 5° poleward of this temperature maximum (Figure 1). This is a generous definition of the monsoon

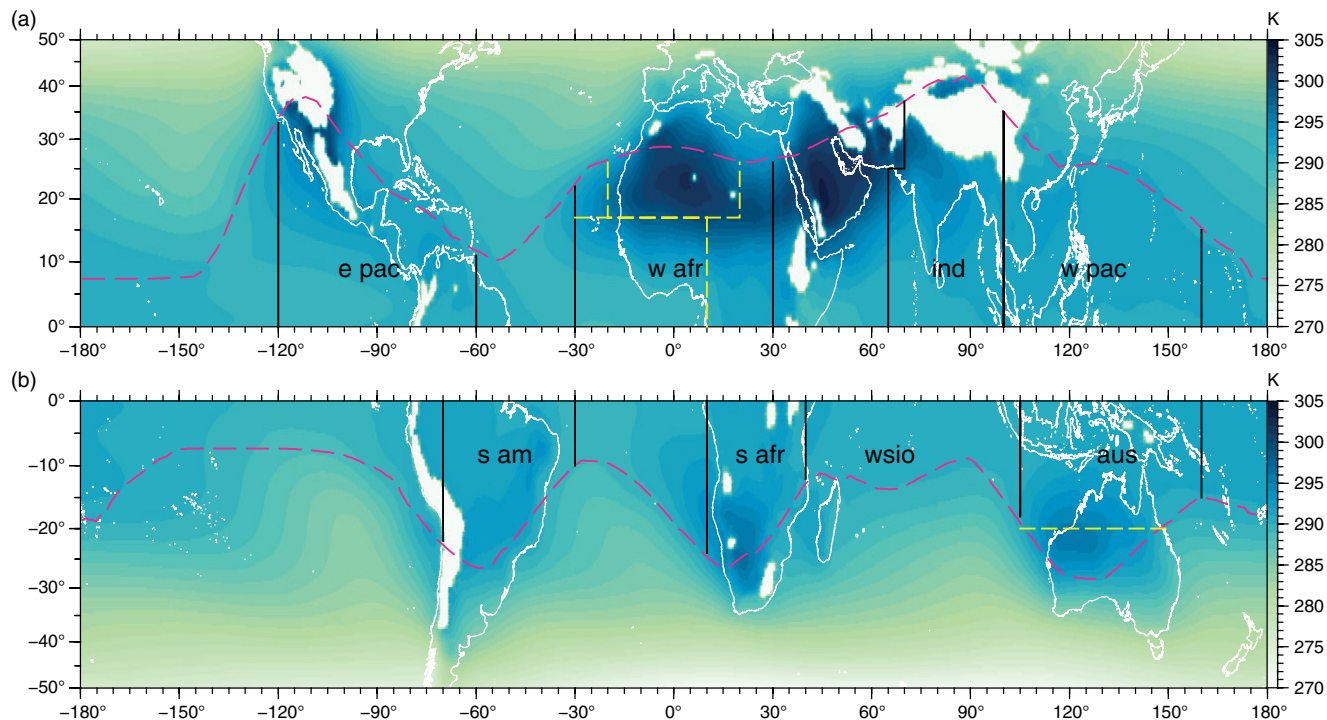


Figure 1. Summer mean (1979–2012) 850 hPa temperature (shading), masked in white where the summer mean 850 hPa surface is below the land surface. The thick dashed line (magenta in online) lies 5° latitude poleward of the 850 hPa temperature maximum at each longitude. (a) Northern (JJA) and (b) Southern (DJF) Hemisphere summer mean. Vertical black lines delineate the western and eastern boundaries of regional monsoon domains, which are latitudinally bounded by the Equator and the dashed magenta line. The thin dashed lines (yellow in online) delineate desert and rain-band subdomains in the western Africa and Australia regions.

domain that allows for the fact that the temperature maximum in the lower troposphere is almost always located further poleward than the temperature maximum in the upper troposphere (e.g. Nie *et al.*, 2010). In effect, this includes in our domain the deserts that are located immediately poleward of most monsoon regions and are known to be associated with synoptic activity (e.g. African easterly waves). Only low-pressure systems at least two days in duration are considered. Regional climatologies, interannual variability and composite structures are presented for the regional monsoon domains that are shown in Figure 1. To be clear, the global monsoon domain used here encompasses a wide variety of mean states, including dry desert regions and oceanic intertropical convergence zones (ITCZs), together with classical monsoon precipitation maxima. This is consistent with the fact that synoptic-scale monsoon disturbances are observed in a similarly wide range of mean states. This domain includes the eastern Pacific ITCZ, which is not commonly thought of as a monsoon but which is included in the monsoon domain of Wang and Ding (2006). The off-equatorial nature of this ITCZ may produce similar synoptic-scale dynamics to those seen in classical monsoon regions; retaining it in our analysis also allows the North American monsoon region to be easily included.

The magnitudes of mean sea-level pressure anomalies and surface wind speed maxima are used to categorize the storms as either monsoon lows or monsoon depressions. Storms more intense than monsoon depressions are placed in a single category consisting of deep depressions and stronger storms. This categorization follows a commonly used set of criteria that is listed in Table 1. While the current definitions of the IMD use only the maximum sustained surface wind speed as a criterion for categorizing low-pressure systems (IMD, 2003), the Sikka archive was compiled based only on surface pressure anomalies (Mooley and Shukla, 1987). Here we use both wind speed and sea-level pressure, as described below.

Mean sea-level pressure anomalies are calculated relative to a 21 day smoothed time series of the mean sea-level pressure field. This reduces the bias that may be introduced from intraseasonal and interannual variability of the mean sea-level pressure field, compared with use of a calendar-based climatological mean. Mean sea-level pressure anomalies and surface wind speeds were

Table 1. Categorization of monsoon low-pressure systems by mean sea-level pressure anomalies and surface horizontal wind speeds. Pressure anomalies are all negative, with values in the table denoting amplitudes.

	Monsoon low	Monsoon depression	Deep depressions and stronger
Mean sea-level pressure anomaly amplitude	≥ 2 hPa	≥ 4 hPa	≥ 10 hPa
Spatial maximum of surface horizontal wind speed	–	≥ 8.5 m s ⁻¹ ≤ 13.5 m s ⁻¹	≥ 13.5 m s ⁻¹

evaluated for each 6 h time step along each track. Tracks were assigned to one of the three intensity categories based on the strongest categorical criteria met simultaneously along the track within the monsoon domain defined above. Sea-level pressure anomaly minima were considered only when they occurred within 500 km of the relative vorticity anomaly and also were defined by closed contours surrounding the vortex centre (i.e. the 850 hPa relative vorticity extremum), with values given in Table 1. Surface wind speed maxima were evaluated only within 500 km of the vortex centre. Note that the ‘monsoon low’ category requires only a pressure anomaly exceeding 2 hPa in amplitude, while the ‘monsoon depression’ category requires a pressure anomaly with amplitude of 4–10 hPa to occur simultaneously with a maximum wind speed of 8.5–13.5 m s⁻¹. The category ‘deep depressions and stronger’ is open-ended and includes all storms stronger than a monsoon depression; hereafter we refer to storms in this category as ‘deep depressions’ for brevity. This manuscript focuses on monsoon depressions and, to a lesser extent, monsoon lows; a brief summary of the distribution of deep depressions is presented for reference in the Appendix. Again, storms are classified by the most intense category achieved along their track within the monsoon domain, so that a storm that has a peak pressure anomaly of 6 hPa but peak wind speeds of 7 m s⁻¹ is categorized as a monsoon low, since that is the most intense category achieved. Similarly, a storm that achieves depression status within the monsoon domain but intensifies to a deep

depression outside this domain (e.g. in the midlatitudes poleward of the 850 hPa temperature maximum) remains categorized as a depression. This approach is conservative, in that it requires that both sea-level pressure anomaly and wind criteria be met simultaneously along the portion of the tracks that occurs within the monsoon domains. Use of the sea-level pressure anomaly criteria alone yields a dramatically larger estimate of the number of monsoon depressions. For instance, over India 191 tracks meet the sea-level pressure anomaly criteria somewhere along their path during JJAS 1979–2003. For the same period, however, only 99 tracks meet both the sea-level pressure and wind speed criteria simultaneously within the monsoon domain. For reference, the Sikka archive recognizes 61 monsoon depression-strength storms for the same period over the same region. Similarly, using only surface wind speeds for categorization would result in weak vortices being classified as depressions or deep depressions when they drift into a region of high climatological mean wind speed (summer mean surface wind speeds in the Arabian Sea exceed 15 m s^{-1}). No moisture criterion is used in the categorization of low-pressure systems, by intent, so that our results may include both strongly precipitating storms and dry vortices.

From the complete set of monsoon low-pressure systems identified as described above, genesis and track density distributions were computed by calculating the total number of genesis or track positions within a 500 km radius of each grid point. This yields a track density phrased in terms of a unit horizontal area similar to that used by Thorncroft and Hodges (2001) in their study of African easterly waves.

Monthly climatologies and interannual time series of storm counts were constructed for each monsoon region by counting the number of storms per month or year based on the time and location of track genesis. These statistics were compiled for each of the three storm intensity categories.

Composite structures of summer (MJJAS and NDJFM) vortices having monsoon depression intensity were constructed for each region from the ERA-Interim data. Composites were centred on the 850 hPa vortex centre at each track position and averaged over all time steps that met the conditions for monsoon depression intensity. Then the average of all storms within a region was calculated to produce each composite.

3. Results

3.1. Indian monsoon low-pressure systems

We begin by comparing results from our tracking algorithm with those from an inventory previously compiled for the Indian monsoon region, the Sikka archive. The period of overlap for these data is 1979–2003, as ERA-Interim begins in 1979 and the Sikka archive ends in 2003. Also, the Sikka archive considers only the months of June–September, so only those months are considered in this comparison. The genesis distribution maximum for Indian monsoon low-pressure systems (including lows, depressions and stronger storms) is centred over the northwestern Bay of Bengal for both the Sikka archive and ERA-Interim (Figure 2). For the primary genesis region over the Bay of Bengal, the ERA-Interim maximum (~ 6 storms per summer within a 500 km radius) is less than the maximum for the Sikka archive (~ 12 storms per summer within 500 km), but the area over which genesis is focused in ERA-Interim is larger than that of the Sikka archive, so that the area integrals are similar (see below). The broader ERA-Interim genesis distribution likely occurs because our automated algorithms track vorticity anomalies to genesis points that are earlier in time than those identified by subjective analysis of sea-level pressure maps. Indeed, the average ERA-Interim track length for all Indian monsoon low-pressure systems is about 7.5 days, while it is only 5 days for the Sikka archive. Overall, the spatial distribution of ERA-Interim storms for the Indian monsoon region compares well with that of the Sikka archive.

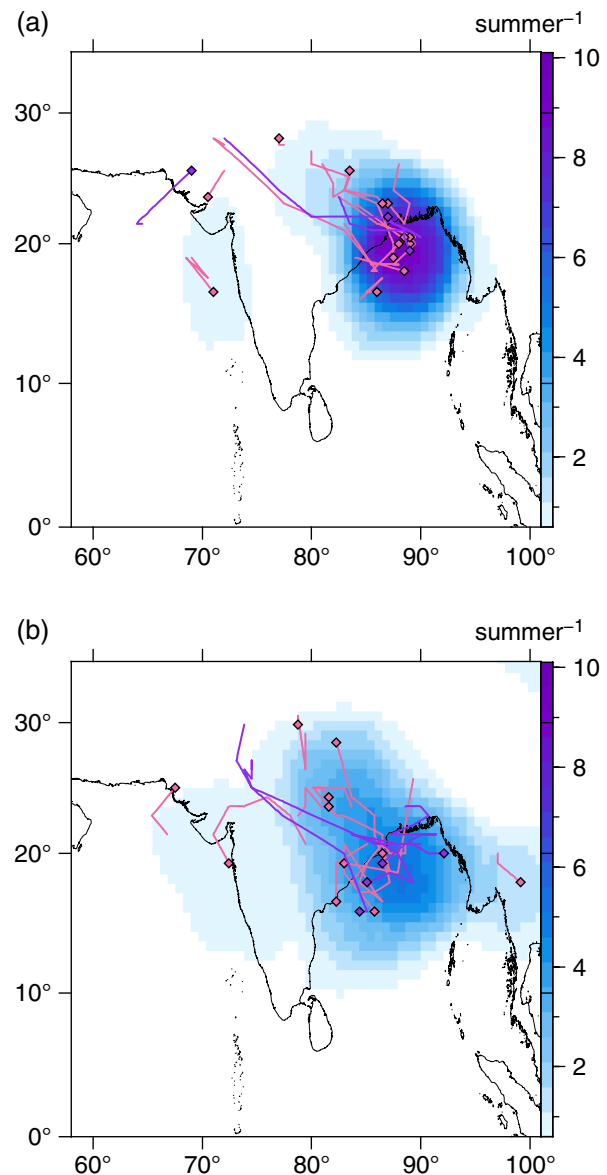


Figure 2. The shading shows the number of monsoon low-pressure system genesis points per summer (JJAS) occurring within a 500 km radius of each grid point from (a) the Sikka archive and (b) ERA-Interim for 1979–2003. Genesis points (filled squares) and tracks (solid lines) are shown for summer 2003, with pink representing monsoon lows and purple representing monsoon depressions.

Composites of daily anomalous precipitation and daily anomalous OLR, relative to a daily climatology, for storms of monsoon depression intensity are presented in Figure 3 (a summer climatology is also shown for reference). These plots show horizontal structures using observations that do not depend on the numerical model used in the reanalysis. Both the Sikka and ERA-Interim composites, like prior precipitation composites for monsoon depressions (Godbole, 1977), have precipitation maxima west/southwest of the vortex centre. The composite precipitation maximum is about 20 mm day^{-1} and the area over which the precipitation occurs is approximately 1000 km in diameter. The composite negative OLR anomaly extends over an area about twice as large as that of the precipitation. The location of the OLR minima roughly coincides with the location of precipitation maxima, as expected for storms with deep convection. However, the OLR anomaly extends further west than the precipitation anomaly, perhaps because the upper-level mean monsoon flow produces westward advection of the high clouds associated with deep convection (Grossman and Garcia, 1990). Daily OLR anomaly minima are about -35 W m^{-2} for the Sikka composite and about -45 W m^{-2} for the ERA-Interim composite. This difference in amplitude likely reflects the fact that the ERA-Interim composites were constructed using data from only those

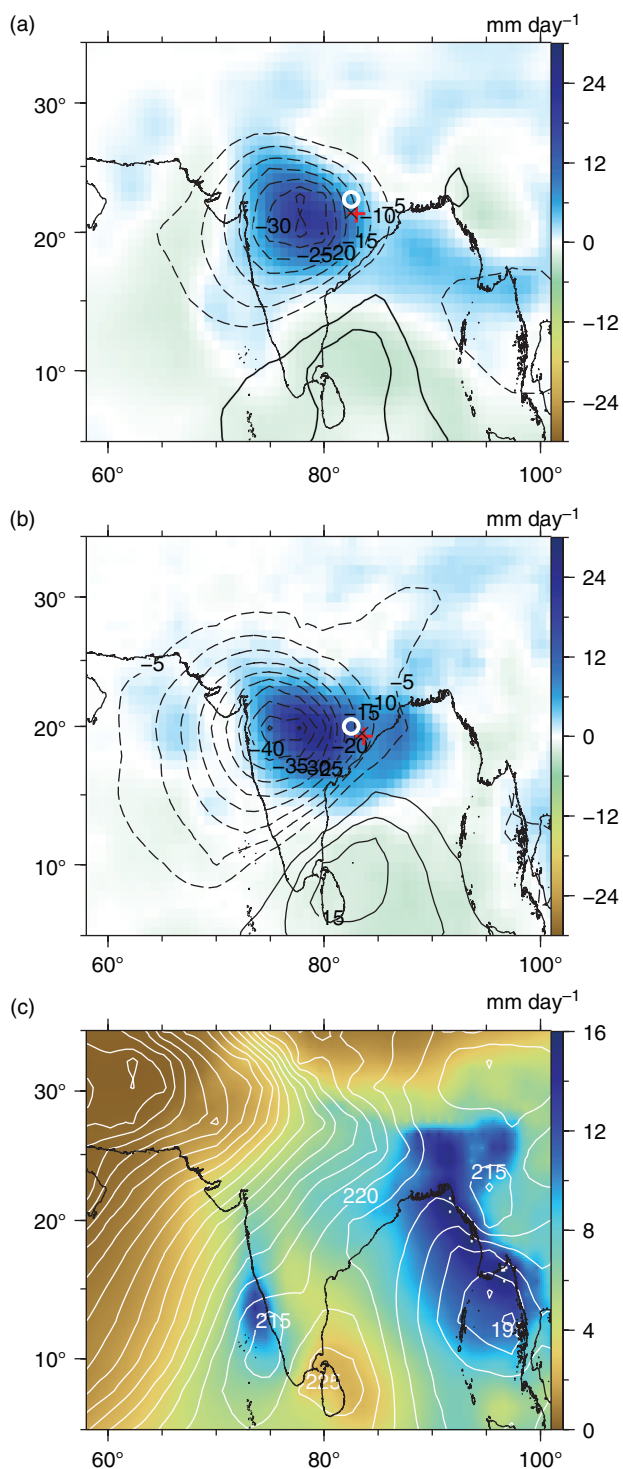


Figure 3. Composite anomalous daily precipitation (shading, GPCP, in mm day⁻¹) and anomalous daily NOAA OLR (contours, in W m⁻²) for Indian monsoon depressions from (a) the Sikka archive and (b) ERA-Interim. (c) Summer (JJA) climatology for daily precipitation (shading) and OLR (white contours). Dashed contours are negative and the contour interval for all plots is 5 W m⁻². The red '+', the black 'X', and the white circle represent the grid point closest to the vortex center in the ERA-Interim, precipitation and OLR data sets, respectively.

days when the track met the criteria for a depression. These results indicate that monsoon depressions identified from ERA-Interim are not artefacts of the reanalysis; they have horizontally extensive areas of cloud cover and precipitation, with spatial structures consistent with previous studies.

The location of peak precipitation west of the vortex centre is expected from previous theory. Ascent and thus precipitation are expected to occur on the downshear side of a vortex due to quasi-geostrophic dynamical lifting (e.g. Sutcliffe, 1947; Trenberth, 1978). Since the vertical wind shear is easterly in monsoon regions,

peak precipitation is therefore expected to occur west of the vortex centre. Consistent with the structures shown in Figure 3, detailed analysis of the quasi-geostrophic omega equation has shown that the peak dynamical lifting is typically west-southwest of the vortex centre for case studies of individual Indian monsoon depressions (Rao and Rajamani, 1970; Daggupati and Sikka, 1977; Saha and Chang, 1983; Sanders, 1984) as well as for a composite of over 100 Indian monsoon depressions (Boos *et al.*, 2014).

According to the Sikka archive, an average of 14 (with a standard deviation of 2.3) monsoon low-pressure systems occur over India each summer in this 25 year period: about 10 lows, 2.5 depressions and 1.5 deep depressions (Figure 4(b)). From ERA-Interim, we detect about 16 (with a standard deviation of 2.4) monsoon low-pressure systems per summer over the same years: 12 lows, 4 depressions and fewer than 1 deep depression (Figure 4(d)). The Sikka archive has the most frequent low-pressure system genesis in August, while the ERA-Interim peak is in July and monthly totals decrease for the remainder of the summer (Figure 4(a) and (c)). There seems to be little correlation between interannual variations in the two track collections; this is perhaps not surprising, given the large differences in the underlying observational datasets and the methods of vortex detection and tracking (e.g. the Sikka archive detected low-pressure systems based only on surface pressure, while our methodology used 850 hPa vorticity, surface wind speed and sea-level pressure). It has recently been shown that the number of tropical cyclones detected in numerical models can vary by an order of magnitude depending on the details of the algorithm used for tracking (e.g. Suzuki-Parker, 2012). Even when an automated algorithm that used only surface pressure was used to detect and track Indian monsoon low-pressure systems in two reanalysis products, the interannual correlation between the objectively derived storm counts and counts from the Sikka archive (which was also derived using surface pressure) was only 0.3–0.6 (V. Praveen, S. Sandeep, R. S. Ajayamohan, 2014; personal communication). Thus, we do not consider deviations in our interannual variations from those in the Sikka archive to be indicative of a major flaw in our methodology. The general similarity of our track distributions and storm structures with those from the Sikka archive lends confidence that our algorithms are detecting and categorizing storms in a way consistent with previous studies of Indian monsoon low-pressure systems.

3.2. Genesis and track density distributions

Extended summer (MJJAS and NDJFM) climatological distributions of genesis for monsoon lows and monsoon depressions are shown in Figure 5, together with tracks for the summer of 2012 (tracks are only shown for one year for clarity). The deep depression category is excluded from the analyses presented in this section, in order to focus attention on synoptic-scale vortices that do not achieve intensities near those of tropical cyclones within the monsoon domain. It should be remembered that vortices are classified by the peak intensity they achieve within the monsoon domain, so that some of our monsoon lows may intensify to hurricanes or typhoons after they leave this domain.

Genesis maxima for lows and depressions generally peak between 10 and 30° latitude in each hemisphere and exhibit more zonal asymmetry than could be produced by asymmetries in the domain specification alone (cf. Figure 1). In the Northern Hemisphere, most monsoon lows originate over northern Africa, with weaker genesis maxima over South Asia, the Middle East and the eastern Pacific ITCZ. Many of the tracks for these storms are short in distance travelled, especially for those originating over land (all storms considered here are at least two days in duration). There is a tendency for long-lived storms to originate near western Africa and from the ITCZ south of Mexico, then migrate to the west-northwest. We show in separate work (Boos *et al.*, 2014) that Indian monsoon depressions propagate to the northwest primarily because of adiabatic beta drift; this process

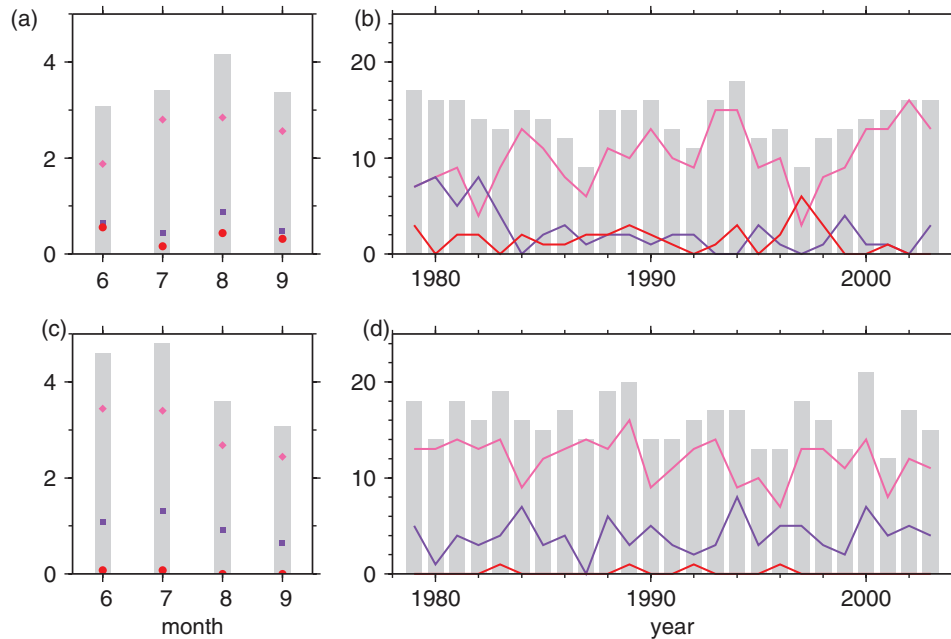


Figure 4. (a,c) Monthly climatology for 1979–2003 and (b,d) yearly time series of the number of Indian summer (JJAS) monsoon low-pressure systems, from (a) and (b) the Sikka archive and (c) and (d) ERA-Interim. Colour corresponds to intensity categories and the grey bars are the total values. Monsoon lows are pink (diamonds), monsoon depressions are purple (squares) and deep depressions and stronger are red (circles).

may act in other regions, presumably with some modification by the local mean wind. Maxima for genesis of monsoon depressions in the Northern Hemisphere occur over the Bay of Bengal, the western Pacific, West Africa and the eastern Pacific ITCZ. In the Southern Hemisphere, maxima for genesis of monsoon lows occur near 25°S over each continent, generally toward the western side of each land mass. Weaker maxima are also found west and east of Indonesia over the southern Indian Ocean. These regions, together with northern Australia and the Gulf of Carpentaria, are also maxima for genesis of monsoon depressions, although far more depression-strength vortices form over Australia than in any other Southern Hemisphere region. Depressions typically migrate initially to the southwest and then veer poleward and to the southeast, perhaps due to beta drift that is modified in the latter part of the track by mean westerly flow.

The previous section showed that our genesis distribution of Indian monsoon depressions compared well with that of a previously compiled archive of Indian monsoon depression tracks; we now briefly reconcile our inventory of monsoon low-pressure systems over West Africa with a previously compiled archive of African easterly wave tracks. Thorncroft and Hodges (2001) estimated the genesis and track densities of African easterly waves, also using the TRACK software but with earlier ECMWF data products and without consideration of sea-level pressure or surface wind speed. From their analysis of the 850 hPa relative vorticity, they identified two genesis density maxima for African easterly waves. The greater of these maxima (~ 7 per 10^6 km² per summer) occurs over the Atlantic, just west of Guinea and Sierra Leone, and the second genesis density maximum (~ 5 per 10^6 km² per summer) occurs over the Algerian Saharan Desert. The track density maxima (about 7–8 per 10^6 km² per summer) from their analysis lie just downstream (i.e. west) of these genesis maxima. From ERA-Interim, we also identify a genesis density maximum (~ 10 per 0.785×10^6 km² per summer) over the Algerian Saharan Desert, with a secondary maximum (~ 7 per 0.785×10^6 km² per summer) southwest of there over Mauritania and Mali. Unlike Thorncroft and Hodges (2001), we do not identify a genesis maximum west of the African coast over the eastern Atlantic Ocean. However, our summer (MJJAS) track densities just west of Africa (Figure 6(a)) are similar to those of Thorncroft and Hodges (2001). ERA-Interim has about ten monsoon low-pressure systems that track through the region west of the coast of Guinea in an average summer, compared with Thorncroft

and Hodges' count of about 8.2 storms per summer for the same region. This suggests that our methodology and data allow vortices to be tracked further upstream to origins over the African continent. This may be a function of the higher resolution of ERA-Interim, compared with the T42 resolution of the earlier reanalysis product used by Thorncroft and Hodges, or could be related to different model physics or data assimilation.

Some of the regions of frequent genesis shown in Figure 5 might extend further poleward if we did not limit our dataset to storms that pass through a prescribed monsoon domain. The bounds shown in Figure 1 indeed correspond well with the poleward edges of the regions of frequent genesis of monsoon lows, which indicates that the genesis of weak vortices may not fall off as precipitously with latitude as one might naively infer from Figure 5(a) and (b). However, the genesis distributions for depressions exhibit much more spatial structure than can be explained by a simple truncation of an otherwise spatially homogeneous distribution. The consistency of these genesis distributions with previous studies (e.g. Thorncroft and Hodges, 2001; Sikka, 2006) also shows that the genesis distributions for depressions are likely not strongly influenced by our choice of monsoon domain. The Australian genesis distribution produced by Berry *et al.* (2012) lacked the strong maximum over western Australia that dominates our Southern Hemisphere distributions; this is likely a result of our different selection criteria and is discussed below in the context of composite structures.

3.3. Monthly climatologies and time series

Monthly climatologies and interannual variability of monsoon low-pressure systems were determined for the regional monsoon domains shown in Figure 1. These regions were selected to document the variability and composite structures of storms, particularly those of monsoon depression intensity, at locations of genesis and track density maxima (Figures 5(c) and (d) and 6). In the Northern Hemisphere, these regions are India, the western Pacific, West Africa and the eastern Pacific. In the Southern Hemisphere, these regions are Australia, the western southern Indian Ocean, southern Africa and South America. The number of monsoon low-pressure systems per boreal summer in the Northern Hemisphere is two to three times that in the Southern Hemisphere during austral summer (Figures 7 and 8). For the category of monsoon depressions (denoted by purple in Figures 7

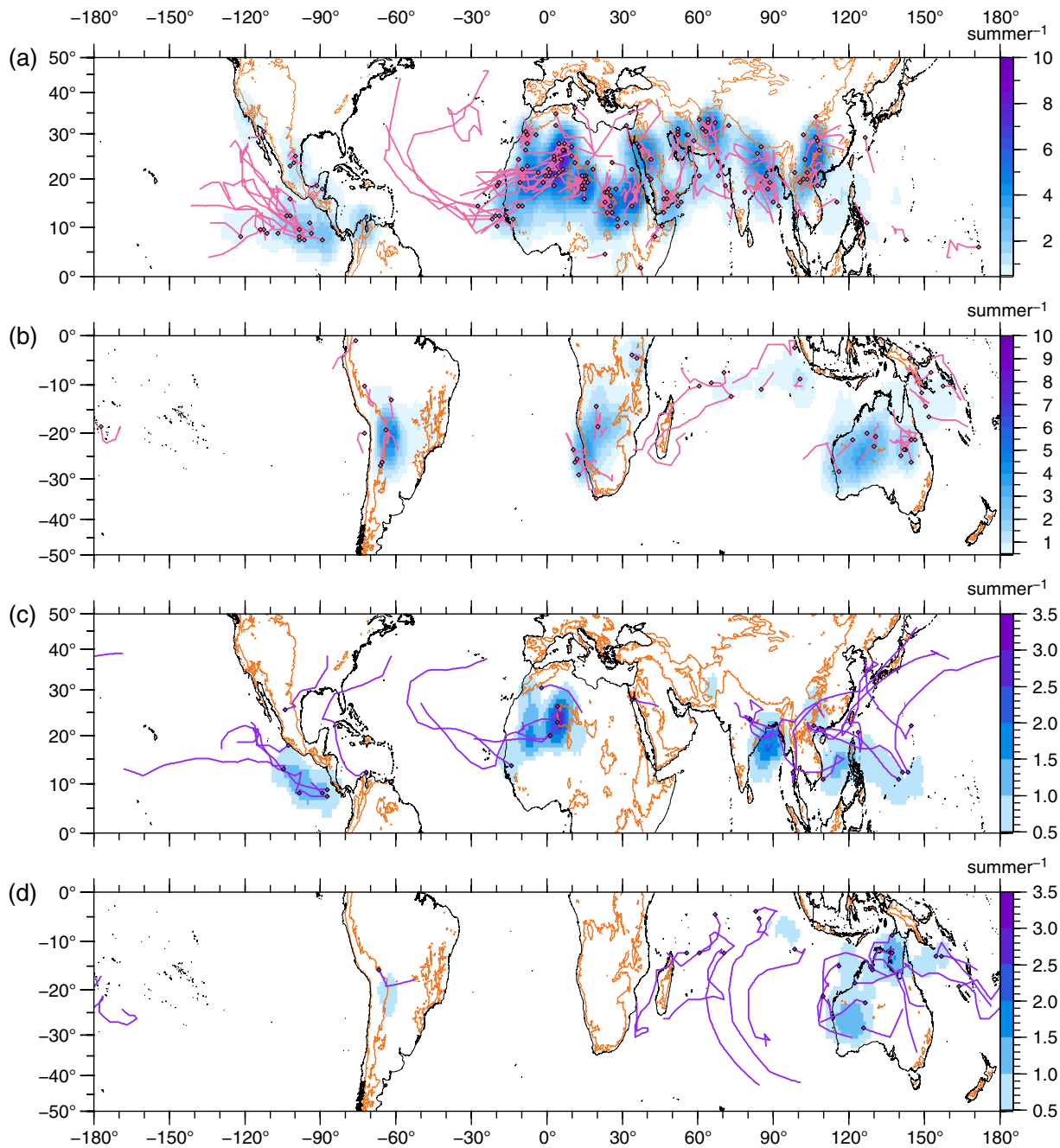


Figure 5. Hemispheric distributions of genesis and tracks for monsoon low-pressure systems from ERA–Interim for local summer (MJJAS and NDJFM). Shading indicates the average number of genesis positions occurring per summer within a 500 km radius of each point during 1979–2012. Tracks and genesis positions for summer 2012 are indicated by the solid lines and filled diamonds. (a,b) Monsoon lows and (c,d) monsoon depressions. Brown contours are the 800 m surface elevation. Note the change in colour scales between panels.

and 8), about 30–40 storms occur per summer in the Northern Hemisphere, compared with about 15 south of the Equator during austral summer. In general, low-pressure systems of all categories form most often during local summer, although genesis occurs during all seasons in every region. Note that Figures 7 and 8 include monthly climatologies for the full year based on the time period 1979–2012 (left columns) and interannual time series of counts for extended summer periods (MJJAS and NDJFM, right columns). This presentation contrasts with the results shown in Figure 4 (for JJAS, 1979–2003), as that figure was designed to compare in a consistent manner the Sikka archive and the ERA-Interim results.

In most regions, there is a stratification of frequency by categorical intensity, with lows being more common than depressions, often by a factor of 2–3 or more. This stratification is not as pronounced over the western Pacific, where monsoon depressions are nearly as frequent as monsoon lows during local summer. The number of depressions is also nearly equal

to the number of lows during some years in Australia and the southwestern Indian Ocean. While we do not examine the mechanisms or statistical associations of interannual variations in the time series shown in the right-hand columns of Figures 7 and 8, it is noteworthy that the magnitude of interannual variability is only about 8–10% of the long-term mean. Thus, the genesis distributions shown in Figure 5 are generally representative of the regional storm counts that occur every year.

3.4. Composite structures

To assess and compare the regional structures of monsoon depressions, composites were developed for each region from reanalysis winds, potential temperature and PV. Indian monsoon depressions have been previously characterized by a tilt in the vertical to the west and south, a warm over cold temperature anomaly in the storm centre, peak horizontal winds around 700–800 hPa and cyclonic winds extending from the surface

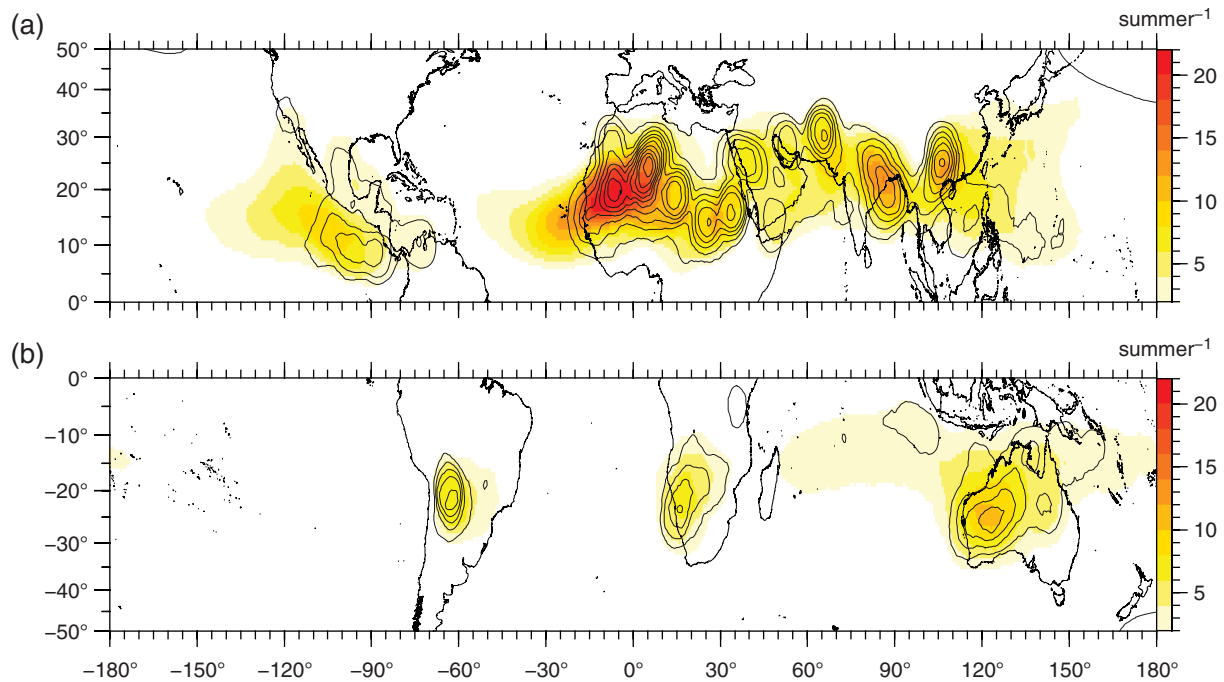


Figure 6. Track and genesis density distributions for monsoon low-pressure systems from ERA–Interim (1979–2012) in (a) Northern Hemisphere (MJJAS) and (b) Southern Hemisphere (NDJFM). Shading indicates the average number of storm tracks to pass within a 500 km radius of each point per summer. Contours are the average number of genesis positions within a 500 km radius of each point per summer, with a contour interval of 1 summer⁻¹. Values are for the sum of monsoon lows and monsoon depressions. Note the different colour scales in (a) and (b).

to the upper troposphere (Godbole, 1977; Krishnamurthy and Ajayamohan, 2010). The results obtained here for India from ERA–Interim are in agreement with these earlier findings (Figure 9(a) and (b)). Additionally, we find that Indian monsoon depressions consist of deep columns of PV extending from the surface to the upper troposphere, with a PV maximum at around 500 hPa and a secondary, weaker maximum around 850 hPa (Figure 9(b)). The relative vorticity peaks in the lower troposphere (not shown) and the large magnitude of mid- and upper-level PV primarily represents enhanced stratification at those levels. A more detailed discussion of PV in Indian monsoon depressions can be found in Boos *et al.* (2014).

Composite structures of monsoon depressions from the western Pacific (Figure 9(c) and (d)) and Australia (Figure 10(a) and (b)) share these characteristics. Mechanisms of growth and propagation that have been proposed for Indian monsoon depressions may thus also be relevant in those regions (see section 4 for further discussion). Due to the scale of Figures 9 and 10, the characteristic west–southwest tilt with height is not so clear, but it is present for India though not for the other regions. Monsoon depressions from West Africa do not resemble Indian monsoon depressions and are instead warm and shallow (Figure 9(e) and (f)). They have a PV maximum just above the surface, a secondary, weak maximum around 450 hPa and near-zero PV elsewhere in the troposphere. Although this composite structure may be dominated by the large number of dry vortices that exist over the Sahara, composite structures for monsoon depressions originating south of the Sahel, in the ‘rain band’ of West Africa, share similar features (Figure 11(a)–(d)); the regions for which these composites were constructed are indicated by the yellow dashed lines in Figure 1, with the desert domain north of 17°N and the rain band domain equatorward of 17°N). Eastern Pacific ITCZ depressions have a similar PV structure to Indian monsoon depressions, with PV maxima at 500 and 800 hPa, and also have a similar upper-tropospheric warm core. However, their lower troposphere is warm just above the surface and cold at 800 hPa, with these temperature anomalies confined to their poleward side. Monsoon depressions over the southwestern Indian Ocean also have a deep, bimodal PV structure but lack a cold anomaly in the lower troposphere, perhaps indicating greater similarity to traditional warm-core tropical cyclones. Depressions over

southern Africa and central South America are both characterized by nearly horizontal PV structures that extend to the west of the vortex centre. These populations of depressions exist very close to topography, so it is likely that these structures are associated with the dynamics of the low-level topographically trapped winds that exist near the Andes and the plateaus of southern Africa. Reason and Steyn (1990) review a variety of coastally trapped disturbances that are observed along the coastal mountains of southern Africa, South America and other regions. The temperature structure of southern Africa depressions (Figure 10(e)) is shallow, with the warm anomaly confined between the surface and 700 hPa. Potential temperature anomalies in South American depressions consist of a meridional dipole that implies local enhancement of the meridional temperature gradient, perhaps indicative of an association with midlatitude baroclinic waves.

Further analysis of Australian monsoon depressions reveals that composite structures over northern Australia are deep and similar to those of Indian monsoon depressions, but structures over western Australia’s desert regions have more in common with the shallow, warm West African systems (Figure 11(e)–(h)). The regions for which these composites were constructed are indicated by the yellow dashed lines in Figure 1; the desert domain is poleward and the rain-band domain is equatorward of 20°S. The cyclonic PV features associated with the systems over western Australia are confined at such low levels that they would not be captured by tracking algorithms based on PV at 850 hPa or a similarly positioned isentropic level; this likely explains the absence of the western Australian maximum in the genesis distribution produced by Berry *et al.* (2012), which was based on isentropic PV.

3.5. Precipitation attribution

Previous studies have estimated the fraction of precipitation associated with monsoon low-pressure systems in India (e.g. Yoon and Chen, 2005), Australia (Berry *et al.*, 2012) and West Africa (e.g. Mathon *et al.*, 2002; Fink and Reiner, 2003). Here we provide an estimate of the fraction of summer (MJJAS and NDJFM) precipitation that can be attributed to monsoon low-pressure systems. In contrast to previous studies, which were confined to particular regions, we provide a global geographic

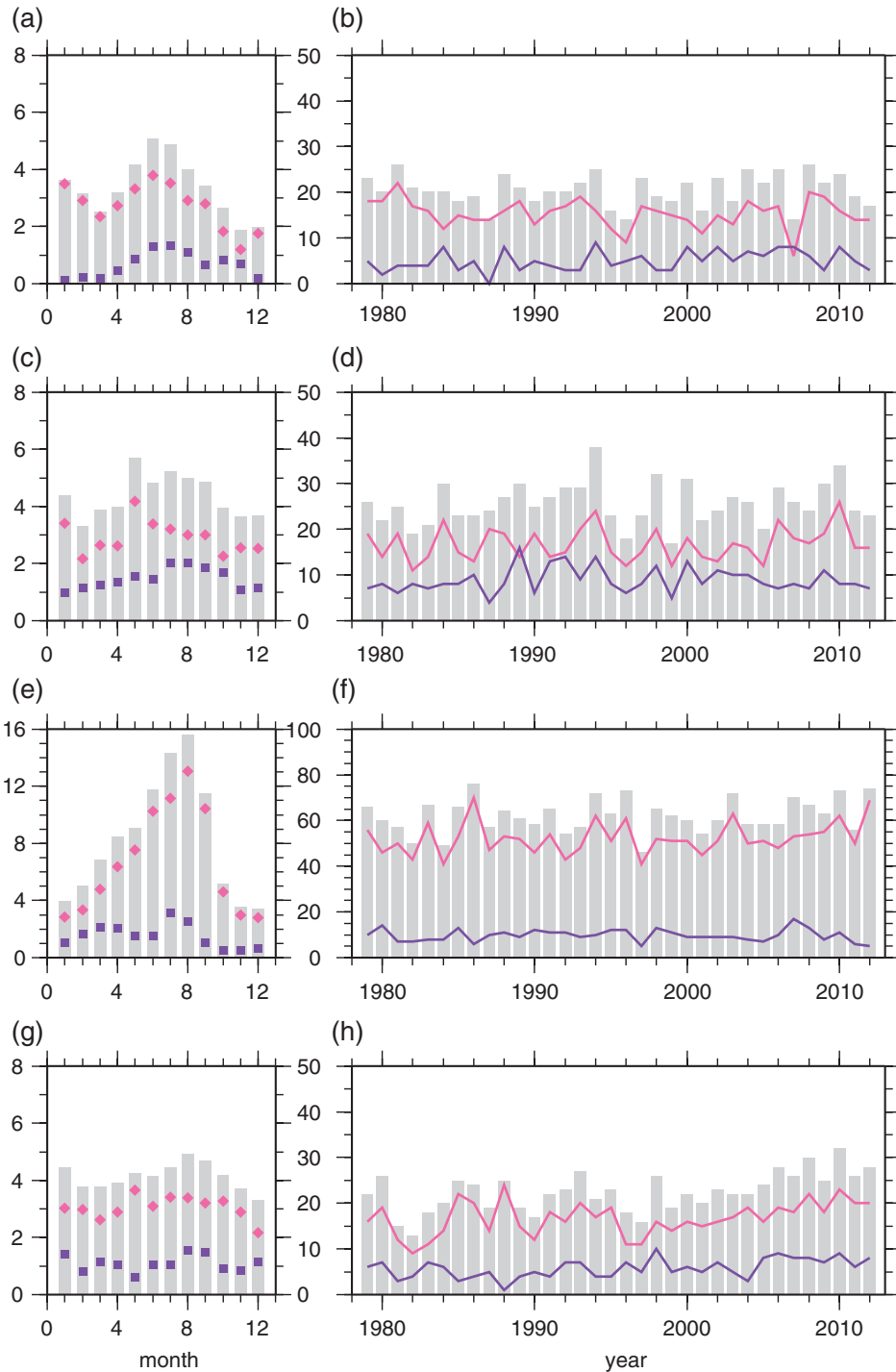


Figure 7. Northern Hemisphere regional monthly climatology ((a,c,e,g, 1979–2012) and time series for summer (MJJJAS, (b,d,f,h)) of the number of monsoon low-pressure systems from ERA–Interim. (a) and (b) India, (c) and (d) western Pacific, (e) and (f) West Africa and (g) and (h) eastern Pacific Intertropical Convergence Zone. Colours correspond to intensity categories and the grey bars are the total values. Monsoon lows are pink (diamonds) and monsoon depressions are purple (squares).

distribution of this fraction. We present both a conservative estimate assuming that all precipitation falling within a radius of 500 km around the vortex centre is associated with the low-pressure system (Figure 12(a) and (b)) and a less conservative estimate using a radius of 1000 km (Figure 12(c) and (d)). The sum of daily precipitation values within the specified radius of the 0000 UTC track position was calculated for all tracks of monsoon low intensity and stronger. Also shown in these figures, for reference, is the summer climatological mean precipitation (solid contours, 5 and 10 mm day⁻¹) and dry zones (dashed contours, 0.5 mm day⁻¹).

From these figures, it is evident that monsoon low-pressure systems account for a large fraction of summer precipitation on the poleward side of the climatological mean precipitation maxima. This large fraction ranges between about 40 and 80%,

depending on the radius used to associate precipitation with a low-pressure system, and is similar across all of the Northern Hemisphere monsoon regions and Australia. The fraction is lower in South America and southern Africa, where it peaks around 40%, although even in those regions this peak fraction occurs on the poleward side of the climatological mean precipitation maximum. The contribution of low-pressure systems to total precipitation increases as one moves away from the climatological mean precipitation maxima in those regions (i.e. westward over the Bay of Bengal or to the southwest along the west coast of Australia). A large contribution of low-pressure systems to Indian rainfall is consistent with the concept of a geostrophic monsoon, where the mean monsoon circulation is geostrophic (i.e. non-divergent) and synoptic systems are needed to produce continental precipitation (Xie and Saiki, 1999).

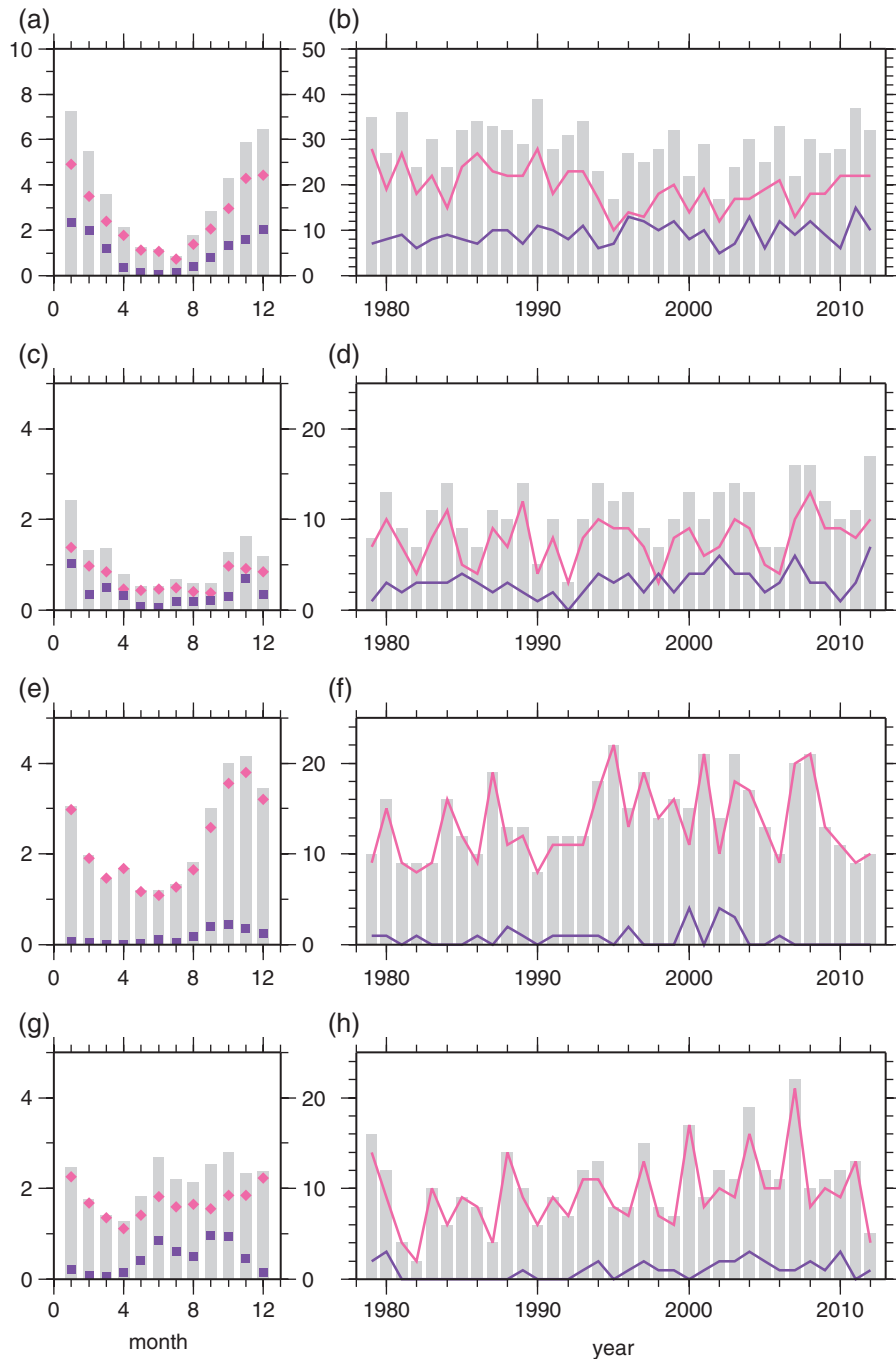


Figure 8. As in Figure 7, but for Southern Hemisphere regions with local summer defined as NDJFM. (a) and (b) Australia, (c) and (d) western southern Indian Ocean, (e) and (f) southern Africa and (g) and (h) South America.

These results generally agree with the regional assessments presented in previous studies, although here we provide a global context and a level of spatial detail that was not previously available. For example, Yoon and Chen (2005) estimated that about half of the summer precipitation over continental India was produced by low-pressure systems, while Berry *et al.* (2012) obtained a similar fraction for northwestern Australia. Thus, while our estimates may be biased high if a substantial amount of precipitation falling within the chosen radii is not associated with a monsoon low-pressure system, the agreement with those previous regional studies suggests this bias is not very large. It is important to note that these fractions are likely an underestimate in regions that lie poleward of our chosen monsoon domain (delineated in Figure 1).

4. Summary and discussion

We have developed a global climatology of monsoon low-pressure systems based on the ERA-Interim reanalysis. Feature tracks were

identified from the 850 hPa relative vorticity field and were then categorized by intensity at six-hourly intervals based on mean sea-level pressure and surface horizontal wind speeds. The spatial distribution of monsoon low-pressure systems in the ERA-Interim reanalysis over India during northern summer agrees qualitatively with that from the Sikka archive. Verification that the Indian monsoon depressions identified from the reanalysis are in fact strongly precipitating convective systems was obtained using satellite-based precipitation and OLR data. Precipitation maxima and anomalous OLR minima occur west/southwest of the low-level vorticity maxima, as expected for vortices in easterly shear (e.g. Sanders, 1984). For India, more monsoon depressions occur in the ERA-Interim reanalysis than in the Sikka archive, about 4 versus 2.5 per summer (JJAS, 1979–2003). However, the Sikka archive has more deep depressions, so this contrast may simply result from different categorization of a small number of storms each year. Another recent analysis (V. Praveen, S. Sandeep, R. S. Ajayamohan, 2014; personal communication), also obtain 4–5 Indian monsoon depressions per summer when using an

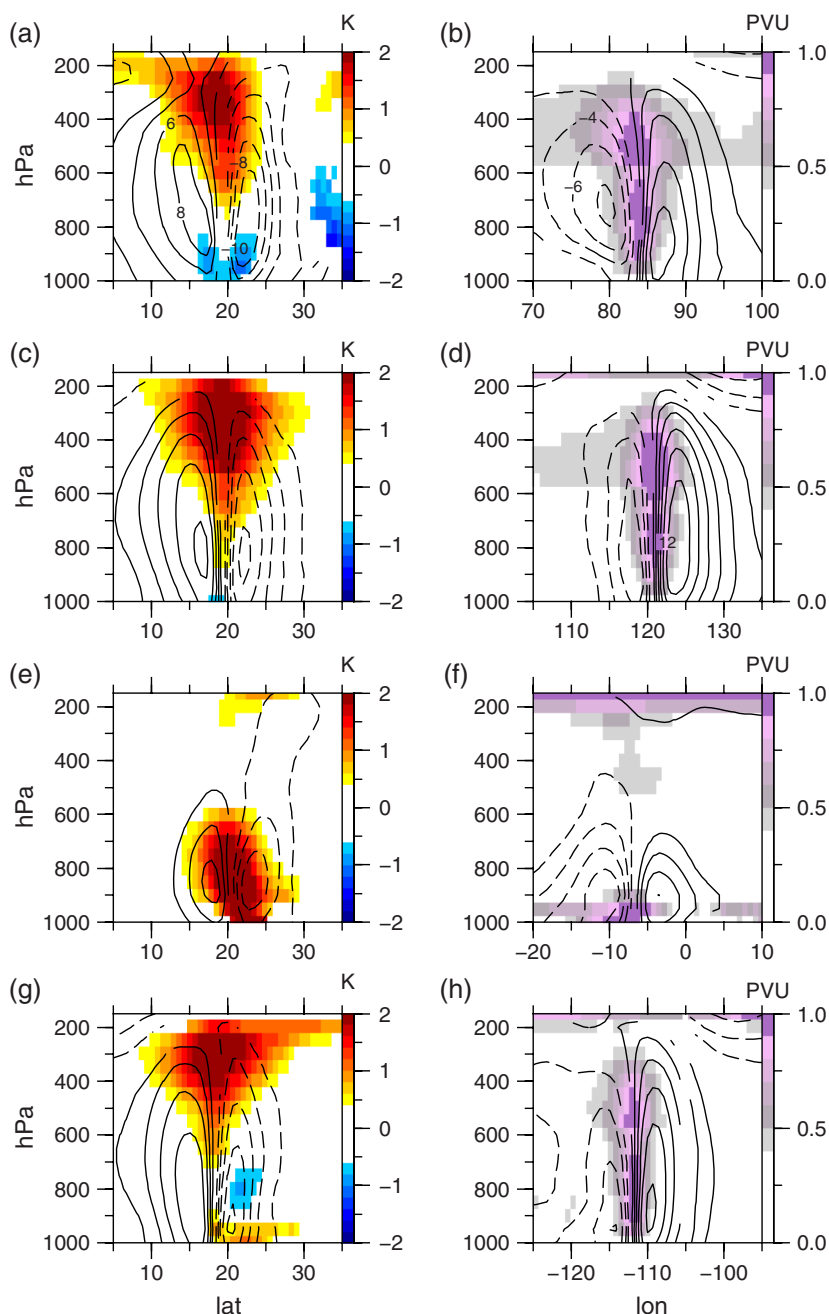


Figure 9. Northern Hemisphere summer (MJJAS) regional composites of monsoon depressions from ERA–Interim (1979–2012). (a,c,e,g) Vertical sections through the storm centre of potential temperature (K, shading) and zonal wind (m s^{-1} , contours; dashed-negative) anomalies. (b,d,f,h) Vertical sections through the storm centre of PV (shading, in PV units (PVU), $1 \text{ PVU} = 10^{-6} \text{ K m}^2 \text{ kg}^{-1} \text{ s}^{-1}$) and meridional wind (m s^{-1} , contours). (a) and (b) India, (c) and (d) western Pacific, (e) and (f) West Africa and (g) and (h) eastern Pacific ITCZ. Dashed contours are negative. Values are shaded or contoured only if by *t*-test they are significant at the 5% level.

automated algorithm to detect low-pressure systems over the Bay of Bengal in two different reanalysis products.

Roughly two to three times as many monsoon low-pressure systems occur in the Northern Hemisphere as in the Southern Hemisphere during local summer. The most frequent genesis generally occurs off the Equator, poleward of 10° latitude in each hemisphere. We speculate that genesis is enhanced in off-equatorial regions because the ambient absolute vorticity is larger there and can thus be more easily concentrated into intense vortices. We will explore in a separate work the statistical relationships between genesis frequencies and properties of the mean state.

Composites of monsoon depressions in India, the western Pacific and northern Australia have a warm-over-cold thermal structure similar to that previously documented in Indian monsoon depressions. Composites in many regions also consist of a column of cyclonic PV that extends from the surface to the upper troposphere, with primary maxima at about 500 hPa and secondary maxima around 850 hPa. This deep, top-heavy

PV structure characterizes monsoon depressions in India, the western Pacific, the eastern Pacific ITCZ, northern Australia and the southwestern Indian Ocean. Boos *et al.* (2014) found that the northwestward propagation of Indian monsoon depressions could be described as an adiabatic nonlinear advection (i.e. beta drift) of the 500 hPa PV maximum. The similarity of the PV fields for depressions in India, the western Pacific and northern Australia suggests that a similar mechanism may govern propagation in those regions. Furthermore, since local PV maxima cannot be created by adiabatic advection, these PV structures indicate the high degree to which diabatic processes must dominate the growth of monsoon depressions. Some previous studies have examined the possible relevance of baroclinic instability to depression growth (e.g. Goswami *et al.*, 1980; Moorthi and Arakawa, 1985; Wang, 1990); the PV structures shown here indicate that any such baroclinic growth process must be highly modified by coupling with moist convection.

Low-pressure systems occupying our depression category over West Africa and western Australia have very distinct structures

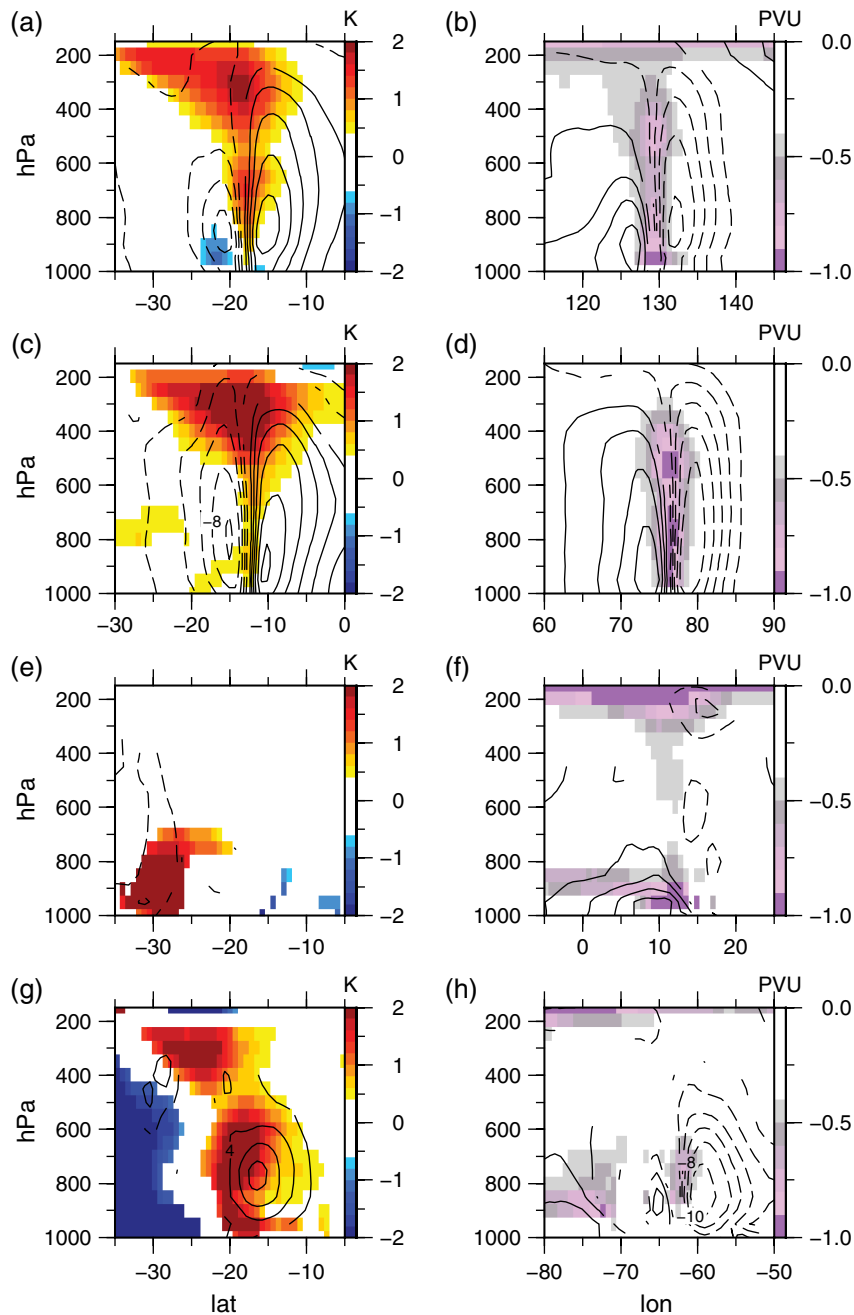


Figure 10. As in Figure 9 but for Southern Hemisphere during local summer (NDJFM). (a) and (b) Australia, (c) and (d) western southern Indian Ocean, (e) and (f) southern Africa and (g) and (h) South America.

that are warm, trapped almost entirely below 500 hPa and are associated with near-surface cyclonic PV maxima. While we have not presented distributions of precipitation or humidity associated with these shallow vortices, they occur over deserts and in a preliminary investigation appear to be a sort of dry, shallow counterpart to the classic precipitation-laden monsoon depression. They are orders of magnitude larger in horizontal scale than microscale dust devils (e.g. Renno, 2008) or mesoscale haboobs (dust storms driven by cold outflow from thunderstorms (Sutton, 1925; Lawson, 1971)). Of greater likely relevance are large-scale heat low circulations, which Racz and Smith (2006) found in an idealized model also to have a warm core in the lower troposphere and a cyclonic PV anomaly trapped near the surface. While this sort of heat low is often viewed as a stationary, climatological mean feature, its associated vorticity and PV could hypothetically be transported by horizontal advection to produce the sort of tracks seen for monsoon lows and depressions over West Africa and western Australia. Previous idealized model studies have found that heat low circulations can interact with background flows to produce diurnally modulated frontogenesis and other deformation of the heat low (Spengler *et al.*, 2005).

Some monsoon low tracks over West Africa and western Australia are so short that they may simply represent slight variations of nearly stationary heat lows, but the depression-strength vortices in these regions generally have tracks that are at least several hundred km in length.

In any case, the nature of these warm and shallow large-scale vortices over West Africa and western Australia merits further investigation. Their population would seem to overlap with that of African easterly waves, although comparison is hindered by the many different criteria used to identify such waves in previous studies. Kiladis *et al.* (2006) identified African easterly waves based on OLR and found vertical structures that extended to much higher levels of the troposphere than in our results. This is not surprising, since selecting for disturbances with low OLR limits the analysis to strongly precipitating systems. Hopsch *et al.* (2012) also found deeper vertical structures for African easterly waves than those produced here, but selected disturbances based on horizontal wind at 600 hPa, which is well above the level at which the circulation of our shallow African systems peaks. Thorncroft and Hodges (2001) selected disturbances based on relative vorticity at either 600 or 850 hPa

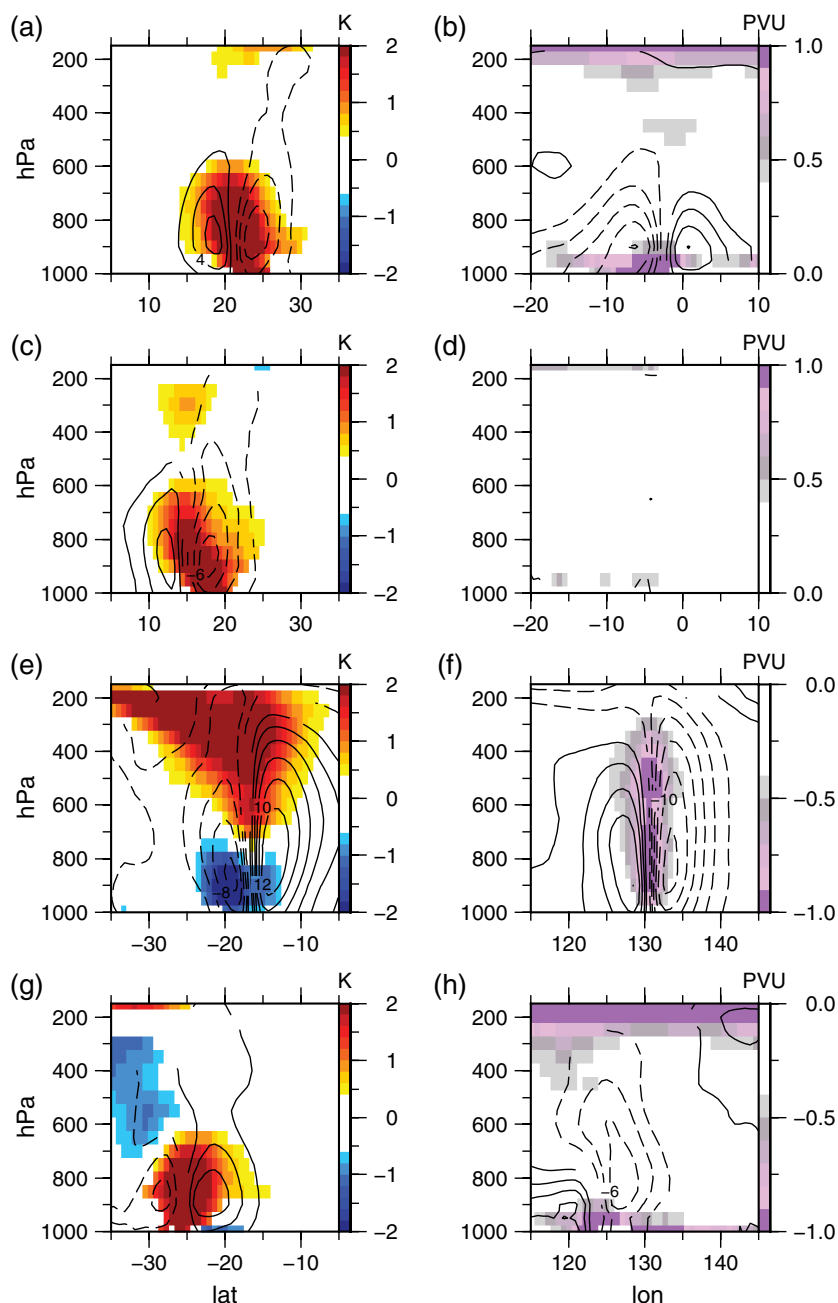


Figure 11. As in Figure 9, but for desert and rain band subdomains in West Africa and Australia. (a) and (b) Rain band West Africa, (c) and (d) desert West Africa, (e) and (f) rain band Australia and (g) and (h) desert western Australia.

and found that 600 hPa activity dominated rainy areas south of 15°N, while 850 hPa activity dominated the drier Saharan region poleward of that latitude. Lau and Lau (1990) also found that 850 hPa vorticity variance over the southern Sahara consisted of dry disturbances with peak amplitude in the lower troposphere, while a band of variability closer to the Equator was associated with deeper moist disturbances. Our results confirm that deep, precipitating easterly waves may coexist over West Africa with shallow, dry disturbances. The latter seem to have been less studied, despite their potentially important role in local meteorology and global dust uplift and transport. A fair number of monsoon low-pressure systems are also generated in the region of the Pakistan–Afghanistan heat low and may share similar dynamics with the shallow disturbances identified over Africa and Australia. It is important to note that shallow, non-precipitating low-pressure systems over deserts may be poorly observed and thus highly influenced by biases in the numerical model used in the reanalysis. We leave detailed investigation of these dry vortices for future studies.

Analysis of precipitation along the tracks of monsoon low-pressure systems shows that these systems account for a large

fraction, from about 40% to more than 80% depending on the assumed radius of the low-pressure system, of total summer precipitation in regions on the poleward edge of the summer precipitation maxima. Monsoon low-pressure systems are thus centrally important for the hydrometeorology of the Sahel, continental India and the Arabian Sea, the South China Sea, western Australia and the eastern Pacific ITCZ region. Whether variability in the number, propagation speed or other properties of monsoon low-pressure systems plays an important role in the variability of precipitation for these regions merits further study.

We close by discussing the existence of long-term trends in the counts of monsoon low-pressure systems. Recent studies have found a long-term increase in the number of monsoon lows and a decrease in the number of monsoon depressions over India (Ajayamohan *et al.*, 2010). This downward trend in Indian monsoon depression counts is pronounced, from about 8 monsoon depressions each summer from the 1920s–1970s to an average of 2–3 in the past decade or two (Krishnamurti *et al.*, 2013). No such trend is obvious in our ERA-Interim-based time series of the counts of Indian monsoon depressions or

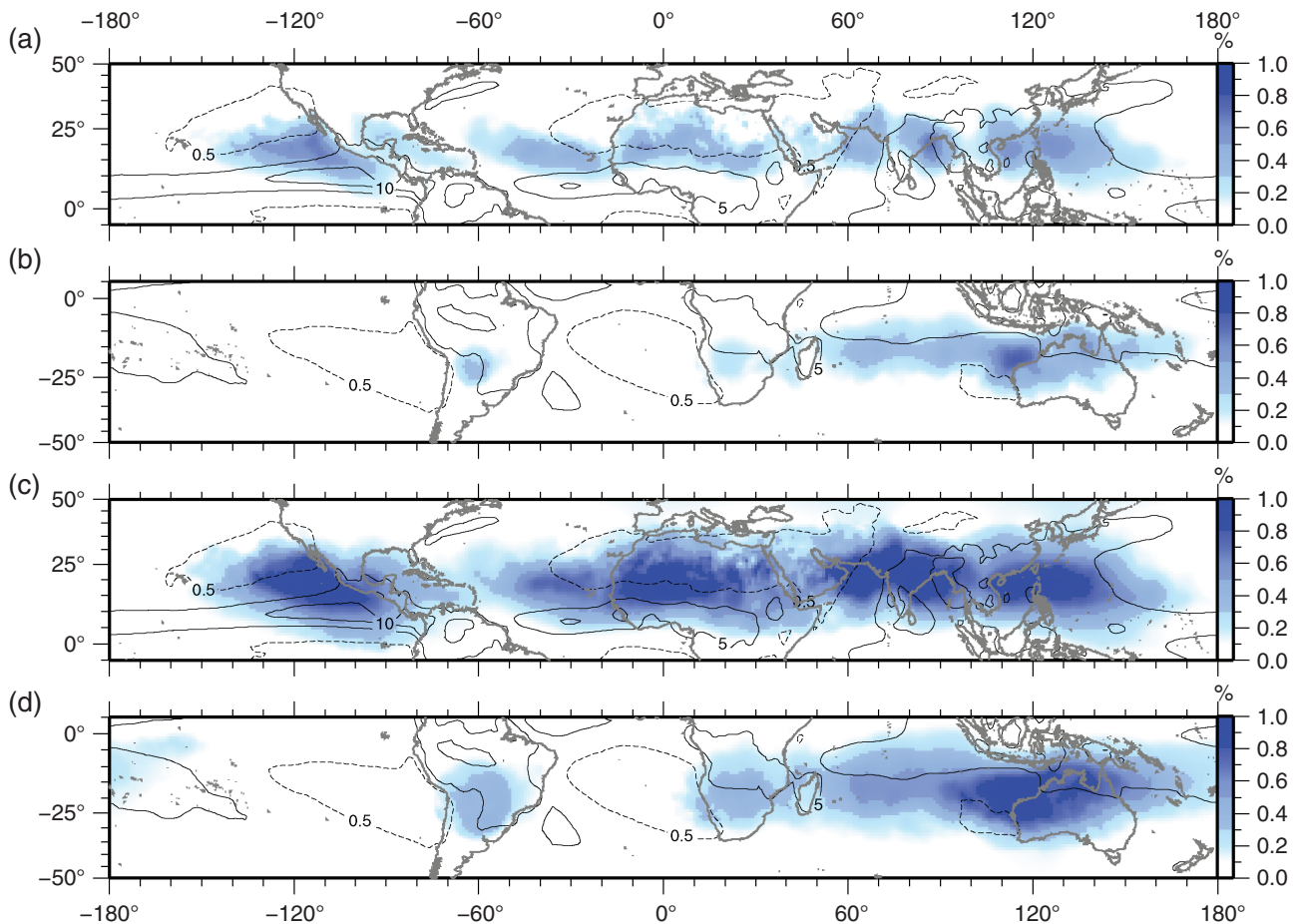


Figure 12. Fraction (shading) of total summer ((a,c) MJJAS and (b,d) NDJFM) precipitation that can be attributed to monsoon lows and monsoon depressions. Shading indicates the ratio of precipitation within (a) and (b) 500 km and (c) and (d) 1000 km of all lows and depressions to the total summer precipitation. Contours reflect the summer climatological precipitation rate. Dashed contours surround dry regions, where precipitation is on average less than 0.5 mm day^{-1} . Solid contours indicate wet regions, where precipitation is greater than 5 mm day^{-1} (5 mm day^{-1} contour interval).

lows (Figures 4(d) and 7(b)). We have purposely refrained from fitting linear trend lines to our data, because of the difficulties inherent in inferring such trends from reanalyses that assimilate data from an evolving observational network. It is possible that the assimilation of larger volumes of satellite data in recent years has led to an under-representation of Indian monsoon low-pressure systems in the earliest decades of ERA-Interim. However, it may also be possible that the subjective identification of monsoon low-pressure systems from evolving operational analyses has introduced spurious trends in the depression counts of the Sikka archive and the India Meteorological Department. We will examine this issue in future work.

Acknowledgement

The ERA-Interim reanalysis was obtained from the Research Data Archive (RDA), which is maintained by the Computational and Information Systems Laboratory (CISL) at the National Center for Atmospheric Research (NCAR). NCAR is sponsored by the National Science Foundation (NSF). The original data are available from the RDA (<http://rda.ucar.edu>) in dataset number ds627.0. GPCP 1° daily precipitation data were obtained from the NASA Goddard Space Flight Center (<http://precip.gsfc.nasa.gov>). NOAA OLR daily data were obtained from the Earth System Research Laboratory at (http://www.esrl.noaa.gov/psd/data/gridded/data.interp_OLR.html). Both authors gratefully acknowledge financial support from Office of Naval Research Young Investigator Program award N00014-11-1-0617 and from National Science Foundation award AGS-1253222. We thank Kevin Hodges for providing the TRACK code and for valuable assistance in configuring that code. We thank Deepthi Achuthavarier for providing the Sikka (2006)

report and Sarah Ditchek for converting that dataset to electronic form. Two anonymous reviewers provided constructive criticism that improved the manuscript. This work was supported in part by the facilities and staff of the Yale University Faculty of Arts and Sciences High Performance Computing Center.

Appendix: Deep depressions and stronger storms

This study focused mostly on storms classified as depressions, and we have not yet discussed the distribution of storms classified as deep depressions (and stronger disturbances). Genesis distribution maxima for deep depressions are focused over oceans, with the most prominent maxima in the western Pacific east of the Philippines and over northern Australia just west of the Gulf of Carpentaria (Figure A1). Genesis also occurs infrequently over the eastern Atlantic and eastern Pacific. Recall that storms are categorized by the peak intensity they achieve within the monsoon domain shown in Figure 1; this prevents many Atlantic hurricanes, for example, from being included in our most intense category. So, while the genesis distribution for our deep depression category may overlap with the genesis distribution for tropical cyclones, tropical cyclones are also expected to be scattered among all of our intensity categories depending on the strength they achieve within the monsoon domain. This may partly explain the lack of a discernible maximum in the genesis distribution for deep depressions in the eastern Pacific, where tropical cyclones frequently form, often from so-called easterly waves in that region's ITCZ. Lack of deep depressions in the eastern Pacific may also be caused by the underrepresentation of tropical cyclone intensities in reanalysis products. Murakami (2014) found that ERA-Interim does underestimate the quantity and intensity of tropical cyclones in the eastern Pacific ITCZ

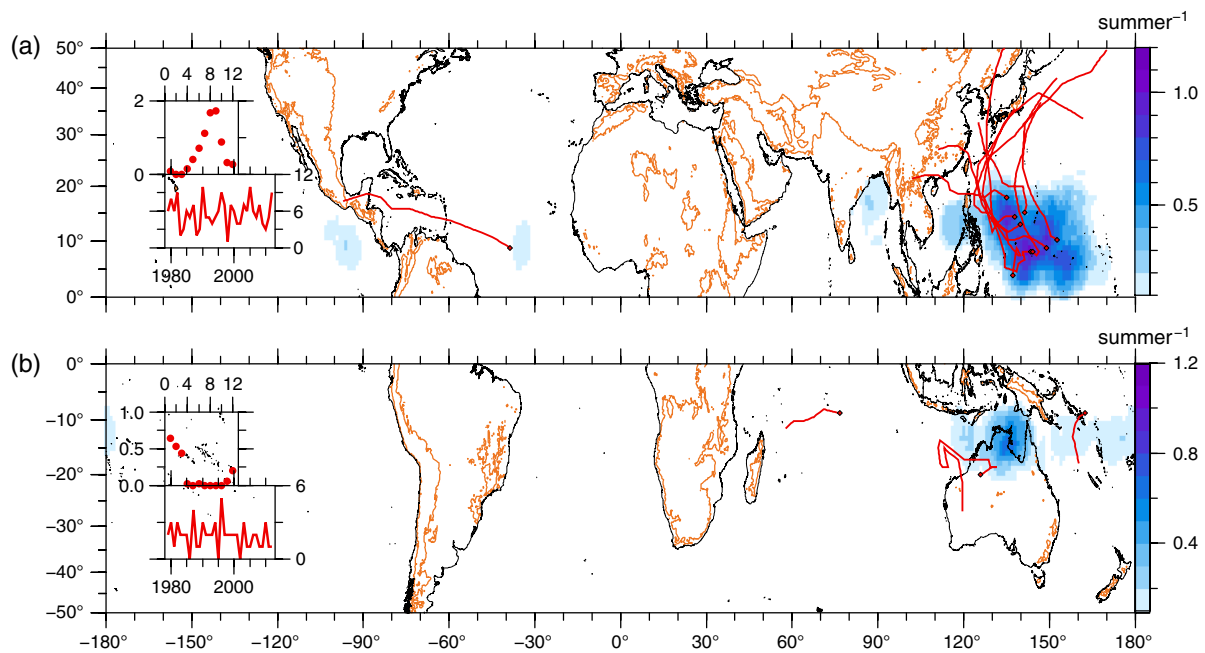


Figure A1. As in Figure 5, but for deep depressions. Insets are monthly climatologies (inset top) and yearly time series (inset bottom) for deep depressions as in Figure 7, for (a) the western Pacific and (b) Australia.

region south of Mexico and that ERA-Interim furthermore exhibited a low correlation (0.14) with observations of interannual variability in the number of eastern Pacific tropical cyclones.

References

- Adler RF, Huffman GJ, Chang A, Ferraro R, Xie P-P, Janowiak J, Rudolf B, Schneider U, Curtis S, Bolvin D, Gruber A, Susskind J, Arkin P, Nelkin E. 2003. The version-2 global precipitation climatology project (GPCP) monthly precipitation analysis (1979–present). *J. Hydrometeorol.* **4**: 1147–1167.
- Ajayamohan RS, Merryfield WJ, Kharin VV. 2010. Increasing trend of synoptic activity and its relationship with extreme rain events over Central India. *J. Clim.* **23**: 1004–1013.
- Aldinger WT, Stapler W. 1998. In *1998 Annual Tropical Cyclone Report*. US Naval Pacific Meteorology and Oceanography Center West/Joint Typhoon Warning Center: Pearl Harbor, HI.
- Baray JL, Clain G, Plu M, Feld E, Caroff P. 2010. Occurrence of monsoon depressions in the Southwest Indian Ocean: Synoptic descriptions and stratosphere to troposphere exchange investigations. *J. Geophys. Res.-Atmos.* **115**: D17108, doi: 10.1029/2009JD013390.
- Beattie JC, Elsberry RL. 2012. Western north Pacific monsoon depression formation. *Weather and Forecasting* **27**: 1413–1432.
- Berry GJ, Reeder MJ, Jakob C. 2012. Coherent synoptic disturbances in the Australian Monsoon. *J. Clim.* **25**: 8409–8421.
- Boos WR, Hurley JV, Murthy VS. 2014. Adiabatic westward drift of Indian monsoon depressions. *Q. J. R. Meteorol. Soc.*, doi: 10.1002/qj.2454.
- Briegel LM, Frank WM. 1997. Large-scale influences on tropical cyclogenesis in the western North Pacific. *Mon. Weather Rev.* **125**: 1397–1413.
- Chen TC, Weng SP. 1999. Interannual and intraseasonal variations in monsoon depressions and their westward-propagating predecessors. *Mon. Weather Rev.* **127**: 1005–1020.
- Daggupaty S, Sikka D. 1977. On the vorticity budget and vertical velocity distribution associated with the life cycle of a monsoon depression. *J. Atmos. Sci.* **34**: 773–792.
- Davidson N, Holland G. 1987. A diagnostic analysis of two intense monsoon depressions over Australia. *Mon. Weather Rev.* **115**: 380–392.
- Dee DP, Uppala SM, Simmons AJ, Berrisford P, Poll P, Kobayashi S, Andrae U, Balmaseda MA, Balsamo G, Bauer P, Bechtold P, Beijaars ACM, Vand Berg L, Bidlot J, Bormann N, Delsol C, Dragani R, Fuentes M, Geer AJ, Haimberger L, Healy SB, Herbach H, Holm EV, Isaksen L, Kallberg P, Kohler M, Matricardi M, McNally AP, Monge-Sanz BM, Morcrette J-J, Park B-K, Peubey C, de Rosnay P, Tavolato C, ThePaut J-N, Vitart F. 2011. The ERA-interim reanalysis: Configuration and performance of the data assimilation system. *Q. J. R. Meteorol. Soc.* **137**: 553–597.
- Eliot J. 1890. *Hand Book of Cyclonic Storms in the Bay of Bengal for the Use of Sailors*. Meteorological Department of the Government of India: Calcutta, India.
- Fink AH, Reiner A. 2003. Spatiotemporal variability of the relation between African easterly waves and West African squall lines in 1998 and 1999. *J. Geophys. Res.-Atmos.* **108**: 1984–2012, doi: 10.1029/2002JD002816.
- Frank NL. 1970. Atlantic tropical systems of 1969. *Mon. Weather Rev.* **98**: 307–314.
- Godbole RV. 1977. Composite structure of monsoon depression. *Tellus* **29**: 25–40.
- Goswami BN, Keshavamurty RN, Satyan V. 1980. Role of barotropic–baroclinic instability on the growth of monsoon depressions and mid-tropospheric cyclones. *Proc. Indian Acad. Sci.-Earth Planet. Sci.* **89**: 79–97.
- Grossman RL, Garcia O. 1990. The distribution of deep convection over ocean and land during the Asian summer monsoon. *J. Clim.* **3**: 1032–1044.
- Hodges KI. 1994. A general method for tracking analysis and its application to meteorological data. *Mon. Weather Rev.* **122**: 2573–2586.
- Hodges KI. 1995. Feature tracking on the unit sphere. *Mon. Weather Rev.* **123**: 3458–3465.
- Hodges KI. 1999. Adaptive constraints for feature tracking. *Mon. Weather Rev.* **127**: 1362–1373.
- Hodges KI, Hoskins BJ, Boyle J, Thorncroft C. 2003. A comparison of recent reanalysis datasets using objective feature tracking: Storm tracks and tropical easterly waves. *Mon. Weather Rev.* **131**: 2012–2037.
- Hopsch SB, Thorncroft C, Tyle KR. 2012. Analysis of African easterly wave structures and their role in influencing tropical cyclogenesis. *Mon. Weather Rev.* **138**: 1399–1419.
- IMD 2003. *Cyclone Manual*. Meteorological Department: New Delhi.
- Kiladis GN, Thorncroft C, Hall NMJ. 2006. Three-dimensional structure and dynamics of African easterly waves. Part I: Observations. *J. Atmos. Sci.* **63**: 2212–2230.
- Krishnamurthy V, Ajayamohan RS. 2010. Composite structure of monsoon low-pressure systems and its relation to Indian rainfall. *J. Clim.* **23**: 4285–4305.
- Krishnamurti TN, Martin A, Krishnamurti R, Simon A, Thomas A, Kumar V. 2013. Impacts of enhanced CCN on the organization of convection and recent reduced counts of monsoon depressions. *Clim. Dyn.* **41**: 117–134.
- Lau KH, Lau NC. 1990. Observed structure and propagation characteristics of tropical summertime synoptic scale disturbances. *Mon. Weather Rev.* **118**: 1888–1913.
- Lawson TJ. 1971. Haboobs structure at Khartoum. *Weather* **26**: 105–112.
- Liebmann B, Smith CA. 1996. Description of a complete (interpolated) outgoing long-wave radiation dataset. *Bull. Am. Meteorol. Soc.* **77**: 1275–1277.
- Mathon V, Laurent H, Lebel T. 2002. Mesoscale convective system rainfall in the Sahel. *J. Appl. Meteorol.* **41**: 1081–1092.
- Mooley DA, Shukla J. 1987. *Characteristics of the Westward Moving Summer Monsoon Low-pressure systems Over the Indian Region and their Relationship with the Monsoon Rainfall*, Technical Report. Center for Ocean-Land-Atmosphere Interactions, University of Maryland: College Park, MD, 218 pp.
- Moorthi S, Arakawa A. 1985. Baroclinic instability with cumulus heating. *J. Atmos. Sci.* **42**: 2007–2031.
- Murakami H. 2014. Tropical cyclones in reanalysis data sets. *Geophys. Res. Lett.* **41**: 2133–2141, doi: 10.1002/2014GL059519.
- Nie J, Boos WR, Kuang Z. 2010. Observational evaluation of a convective quasi-equilibrium view of monsoons. *J. Clim.* **23**: 4416–4428.
- Piddington H. 1876. *Sailor's Horn-Book for the Law of Storms* (6 edn). Williams and Norgate: London.

- Racz Z, Smith RK. 2006. The dynamics of heat lows. *Q. J. R. Meteorol. Soc.* **125**: 225–252.
- Rao KV, Rajamani S. 1970. Diagnostic study of a monsoon depression by geostrophic baroclinic model. *Indian J. Meteorol. Geophys.* **21**: 187–194.
- Reason CJC, Steyn DG. 1990. Coastally trapped disturbances in the lower atmosphere: Dynamic commonalities and geographic diversity. *Prog. Phys. Geog.* **14**: 178–198.
- Reed RJ, Norquist DC, Recker EE. 1977. The structure and properties of African wave disturbances as determined from the ECMWF Operational Analysis/Forecast System. *Meteorol. Atmos. Phys.* **38**: 22–33.
- Renno NO. 2008. A thermodynamically general theory for convective vortices. *Tellus* **60A**: 688–699.
- Sabre M, Hodges K, Laval K, Polcher J, Desalmand F. 2000. Simulation of monsoon disturbances in the LMD GCM. *Mon. Weather Rev.* **128**: 3752–3771.
- Saha K, Chang C. 1983. The baroclinic processes of monsoon depressions. *Mon. Weather Rev.* **111**: 1506–1514.
- Sanders F. 1984. Quasi-geostrophic diagnosis of the monsoon depression of 5–8 July 1979. *J. Atmos. Sci.* **41**: 538–552.
- Sikka DR. 2006. *A Study on the Monsoon Low-pressure systems over the Indian Region and their Relationship with Drought and Excess Monsoon Seasonal Rainfall*, Technical Report No.217. Center for Ocean-Land-Atmosphere Studies, University of Maryland: College Park, MD, 61 pp.
- Spengler T, Reeder MJ, Smith RK. 2005. The dynamics of heat lows in simple background flows. *Q. J. R. Meteorol. Soc.* **131**: 3147–3165.
- Sutcliffe RB. 1947. A contribution to the problem of development. *Q. J. R. Meteorol. Soc.* **73**: 370–383.
- Sutton LJ. 1925. Haboobs. *Q. J. R. Meteorol. Soc.* **51**: 25–50.
- Suzuki-Parker A. 2012. *Uncertainties and Limitations in Simulating Tropical Cyclones*. Springer-Verlag: Berlin.
- Thorncroft C, Hodges KI. 2001. African easterly wave variability and its relationship to Atlantic tropical cyclone activity. *J. Clim.* **14**: 1166–1179.
- Trenberth KE. 1978. On the interpretation of the diagnostic quasi-geostrophic omega equation. *Mon. Weather Rev.* **106**: 131–137.
- Wang B. 1990. On the asymmetry of baroclinic instability between easterly and westerly shear. *Tellus* **42A**: 463–468.
- Wang B, Ding QH. 2006. Changes in global monsoon precipitation over the past 56 years. *Geophys. Res. Lett.* **33**: L06711, doi: 10.1029/2005GL025347.
- WMO. 2011. 'WMO/ESCAP panel on tropical cyclones'. In *WMO/ESCAP Panel on Tropical Cyclones, Thirty-Sixth Session*. Muscat.
- Xie SP, Saiki N. 1999. Abrupt onset and slow seasonal evolution of summer monsoon in an idealized GCM simulation. *J. Meteorol. Soc. Jpn.* **77**: 949–968.
- Yoon JH, Chen TC. 2005. Water vapor budget of the Indian monsoon depression. *Tellus Ser. A-Dyn. Meteorol. Oceanogr.* **57**: 770–782.